ORIGINAL PAPER

Characteristic Impedance and Its Applications to Rock and Mining Engineering

Zong-Xian Zhang[1] · Fengqiang Gong[2] · Elena Kozlovskaya[1] · Adeyemi Aladejare[1]

Abstract

The characteristic impedance of a rock is defined as the product of the sonic velocity and the density of the rock. Based on previous studies, this article finds that: (1) For an intact rock, its characteristic impedance is a comprehensive physical property, since it is closely related with strengths, fracture toughness, Young's modulus, and Poisson's ratio. (2) For rock masses, their characteristic impedances either increase markedly or slightly with increasing depth. (3) The bursts of intact rocks in laboratory are dependent on their characteristic impedances to a great extent, and strong rock bursts happen mostly in the rocks with large characteristic impedance. (4) Rock burst occurrence in tunnel and mines has a close relation with the characteristic impedances of the rocks. (5) Laboratory experiments on different rock samples show that seismic velocity increases as applied stress rises, and field monitored results from coal mines indicate that in the areas where rock bursts happened, the seismic velocity was increasing markedly before or during the bursts. (7) Drillability of rock depends on the characteristic impedance of the rock and the rock with larger impedance has lower drillability or lower penetration rate. (8) The potential applications of characteristic impedance include evaluation and classification of rock masses, and prediction of rock burst proneness and drillability.

Highlights

- Characteristic impedance of rock mass is related to the depth below ground surface.
- Rock bursts are dependent on characteristic impedance of rock.
- Characteristic impedance of rock is related to its strengths, fracture toughness, and Young's modulus.
- Burst proneness and drillability of rock can be predicted by its characteristic impedance.

1 Introduction

Mechanical and physical properties can describe intact rock such as texture, grain size, Young's modulus, Poisson's ratio, porosity, density, compressive strength, tensile strength, shear strength, fracture toughness, hardness, sonic velocities, etc. Here intact rock refers to the unfractured block between discontinuities in a typical rock mass, and it may range from a few millimeters to several meters in size (Hudson and Harrison 1997). The properties concerning intact rock have been well presented in text books such as by Jaeger et al. (2007), Goodman (1989), and Wittaker et al. (1992). However, most intact rock properties are determined in laboratory and their applications to rock and mining engineering are limited due

✉ Zong-Xian Zhang
zongxian.zhang@oulu.fi

Fengqiang Gong
fengqiangg@126.com

Elena Kozlovskaya
elena.kozlovskaya@oulu.fi

Adeyemi Aladejare
Adeyemi.Aladejare@oulu.fi

[1] Oulu Mining School, University of Oulu, Oulu, Finland

[2] School of Civil Engineering, Southeast University, Nanjing, China

to at least three reasons: (1) Rock mass in the field is loaded by in-situ stresses. However, most specimens of intact rock used in laboratory are taken from the field and all in-situ stresses acting on the rock mass have been released. If the in-situ stresses are very high, the rock specimens might have been damaged due to the stress release. (2) Rock mass usually contains geo-structures such as joints and other large discontinuities which affect rock mass properties, but intact rock specimens do not. (3) Rock mass often contains water and sometimes deals with low temperatures (e.g., in cold regions) or high temperatures (e.g., deep mines or deep underground openings), but intact rock specimens in laboratory are often dry and their temperature is usually equal to the room temperature.

To describe and classify rock masses, many methods for rock mass classification have been developed. These methods can be roughly divided into four categories. The first category is the geological classification system that is mainly based on mineral content, texture, mineral size, chemical composition, and origin (sedimentary, igneous, or metamorphic) of rocks (e.g., Bieniawski 1976; Goodman 1989). The second is the engineering classification system that includes several methods such as rock quality designation (RQD) (Deere 1967), tunneling quality index (Q) (Barton et al. 1974), rock mass rating system (RMR) (Bieniawski 1973), geological strength index (GSI) (Hoek et al. 1995), rock mass index (RMI) (Palmstrøm 1996), etc. The third category, to a great extent based on intact rock strength, includes the Protodyakonov index f (see, e.g., Paithankar and Misra 1976; Zou 2017) and the "Three in One Comprehensive Classification System" (Lin et al. 1996) consisting of three components—the point load strength, the specific energy in impact penetration and the sonic velocity of the rock. The fourth category includes relatively new methods using sonic velocity, especially primary wave velocity (P-wave) of rock (e.g., Rawlings and Barton 1995; Zhao and Wu 2000; Nourani et al. 2017; Chawre 2018). The aforementioned methods for classifying rocks have played an important role in rock mechanics and rock engineering, but they have certain drawbacks. For example, the methods in the geological classification system contain little information on mechanical behaviour of rock. The methods in the engineering classification system like RQD, Q, RMI, and RMR often require sample collection, tests of intact rock properties, and extensive field investigations for identifying the frequency and nature of the discontinuities. The methods of the Protodyakonov index and the three in one classification require not only intact rock strength but also other parameters. The methods using sonic velocity are more convenient to implement than other methods, but they have a significant variability in the measured values of rock properties for a given velocity (e.g., Butel et al. 2014; Karakus et al. 2005).

Considering the above drawbacks, a new and feasible system for rock mass classification is still needed.

Characteristic impedance was suggested for evaluation and classification of rock masses, because the characteristic impedance of rock mass could represent the geological structures of the rock mass, e.g., joints, faults, bedding, and mineral composition, to a certain extent (Zhang 2016). Following this suggestion, Zhang et al. (2020a) found six empirical relations between the characteristic impedance and main mechanical properties such as Young's modulus, Poisson's ratio, mode I fracture toughness and uniaxial compressive, tensile and shear strengths of intact rock, based on a great number of intact rock tests. Those relations indicate that characteristic impedance may comprehensively describe the mechanical behaviour of intact rock. On one hand, since intact rock and rock mass are different from each other to a certain extent, it is still a question whether the characteristic impedance of a rock mass is or not able to describe the rock mass comprehensively. On the other hand, since the characteristic impedance of a rock mass can be determined in the field by non-destructive methods, such as geophysics methods, seismic velocity measurements, and muography (Zhang et al. 2020b; Holma et al. 2022), it may have potential applications in mining and rock engineering.

In accordance with the above description, this article investigates how the characteristic impedance of rock mass varies with the depth below the ground surface, how the characteristic impedance of intact rock affects the proneness of rock bursts in laboratory experiments, how the characteristic impedance of rock mass influences the likelihood of rock bursts in tunnels and mines, and whether the drillability of rock can be predicted or not by the characteristic impedance. In addition, this article discusses other potential applications of characteristic impedance in rock and mining engineering.

2 Characteristic Impedance

2.1 Shock Waves

In shock waves, characteristic impedance (Z) is defined as (e.g., Cooper 1996; Zhang 2016)

$$Z = \rho D, \tag{1}$$

where ρ is the density of the material in which a shock wave is propagating and D is the velocity of the shock wave. Notice that D and ρ are variables rather than constants in shock waves. According to one-dimensional shock wave theory, when a shock wave with pressure (P) propagates in a material with zero initial pressure ($P_0 = 0$), we have

$$P = \rho Du, \tag{2}$$

where u is particle velocity. Obviously, in shock waves, the characteristic impedance of a material means the shock pressure caused by per particle velocity in the material. In other words, if a shock wave with a constant particle velocity propagates in two different materials, one having high impedance and the other having low impedance, the shock pressure in the former will be higher than that in the latter.

2.2 Elastic Waves

In elastic waves, characteristic impedance is often called acoustic impedance which is a physical property of material. It is defined as (e.g., Kolsky 1963; Zhang 2016)

$$Z = \rho c, \tag{3}$$

where c is the elastic wave velocity of the material. In the field applications of mining and rock engineering, c should be the P-wave velocity or S-wave velocity of the local rock mass. Elastic wave velocity is also called sonic velocity and it may be either primary wave (P-wave in short) velocity or shear wave (S-wave in short) velocity in the material. Note that in elastic waves, c is constant. In one-dimensional elastic wave problems (e.g., Kolsky 1963; Wang 2007; Zhang 2016), if the initial stress in the material is zero, the stress σ caused by the wave is equal to

$$\sigma = \rho c v, \tag{4}$$

where v is the particle velocity. In the case of P-waves, the stress is either compressive or tensile normal stress, and the wave velocity is P-wave velocity; in the case of S-waves, the stress is shear stress, and the wave velocity is S-wave velocity (Wang 2007). Note that a shear wave may be a torsion wave in a bar or rod. According to Eq. (3), Eq. (4) can be written as

$$\sigma = Zv. \tag{5}$$

Equation (5) indicates that the characteristic impedance of a material means the stress caused by per particle velocity in the material (Zhang et al. 2020a). If the unit of density is kg/m^3 and that of wave velocity is m/s, the unit of the characteristic impedance will be $kg/m^2 s$ and it can be converted to $(N/m^2)/(m/s)$, where N/m^2 is the unit of stress and m/s is the unit of particle velocity. In this sense, if one material has larger characteristic impedance, the stress caused by per particle velocity in the material will be higher, and vice versa. The unit of characteristic impedance can be also converted to $(J/m^3)/(m/s)$, where J refers to joule and J/m^3 is the unit of the energy per volume of material. In view of this unit, the characteristic impedance of a material implies the energy per volume of material caused by per particle

velocity. Correspondingly, if one material has larger characteristic impedance, the energy per volume of material induced by per particle velocity will be more, and vice versa.

2.3 Seismic Waves

In rock engineering and mining engineering, the material in question may be either an intact rock or a rock mass. Such a rock mass may contain various discontinuities and it may be damaged or cracked. Its density might have varied due to in-situ stresses, unloading, or other activities such as mining operations, and its wave velocities measured are often the velocities of seismic waves. Therefore, for engineering applications, the characteristic impedance of a rock mass refers to the product of the density and the seismic wave velocity of the rock mass. Correspondingly, there are two characteristic impedances for a rock mass. One corresponds to P-wave and it is expressed by Z_P, and the other to S-wave represented by Z_S. They are defined as

$$Z_P = \rho V_P \tag{6a}$$

$$Z_S = \rho V_S, \tag{6b}$$

where ρ is the density, V_P is the P-wave velocity, and V_S is the S-wave velocity of the rock mass.

3 Variation of Characteristic Impedance of Rock Mass with Depth Below Ground Surface

Since the characteristic impedance of rock mass is dependent on the density and the seismic velocity of the rock mass according to Eqs. (6a, 6b), the effects of the depth below the ground surface on the density and the seismic velocity are described in the following.

3.1 Density of Rock Mass

Early study by Williamson and Adams (1923) found that the density of the Earth increased with the depth below the ground surface. Later measurements of density log data from many Gulf Coast wells and wells in the Santa Barbara Channel showed that the density of shale mass gradually increased with an increasing depth in those areas (Eaton 1969), as shown in Fig. 1. It can be estimated from Fig. 1 that the density of the Santa Barbara Channel rock at 2000 m depth is larger than that at zero depth (the ground surface) by about 20%. Similarly, the density of the Gulf Coast rock at 2000 m depth is greater than that at zero depth (the ground surface) by around 16%. Such increases in density have a marked impact on the characteristic impedances of the shale

Fig. 1 Shale density vs depth below ground surface. A composite group of density log data were from many Gulf Coast wells and another group of density log data from wells in the Santa Barbara Channel (based on two regressed curves in Eaton 1969)
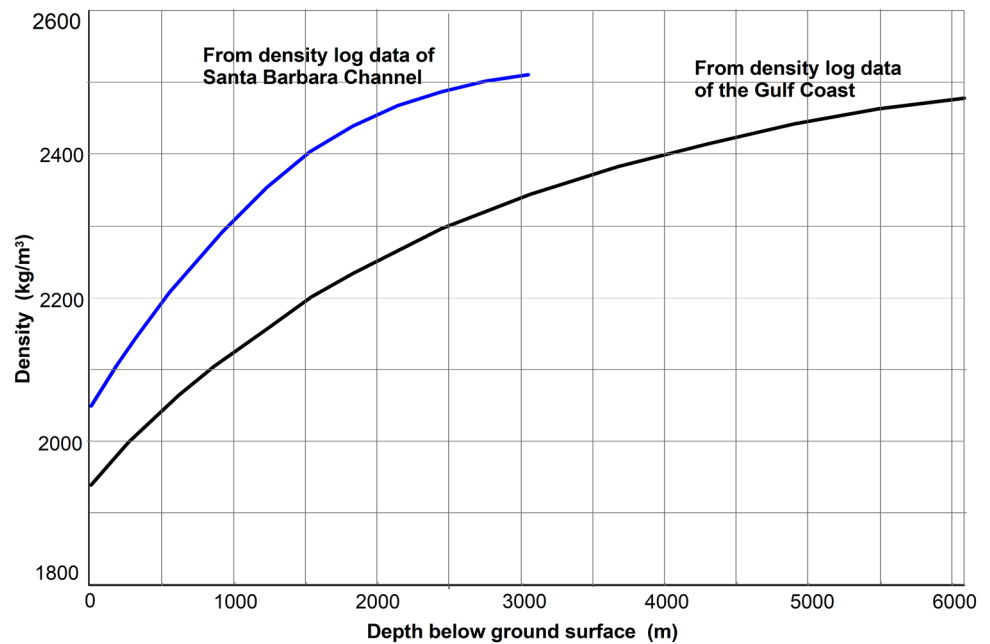
masses. However, note that such increases in the density do not always happen in all rock types. In other words, the densities of some types of rocks do not noticeably increase with increasing depth, for instance, the densities of both metamorphic rocks from the Outokumpu deep drillhole and the Kola superdeep borehole do not markedly increase with increasing depth (Gorbatsevich et al. 2011; Gorbatsevich 2014). This will be discussed in Sect. 4.2.

3.2 Seismic Wave Velocity

Analysis by Williamson and Adams (1923) indicated that P- and S-wave velocities of the Earth increased with increasing depth below the ground surface. Later measurements demonstrated that both wave velocities in different rock masses increased with increasing depth (e.g., Brocher 2008). Brocher (2008) obtained the following empirical equations based on the measurements:

$$V_P = 2.24 + 0.6z \quad \text{Tertiary sedimentary rocks at depth of } 0-4 \text{ km} \tag{7a}$$

$$V_P = 2.75 + 0.47z \quad \text{Great Valley sequence at depth of } 0.05-4 \text{ km} \tag{7b}$$

$$V_P = 2.5 + 1.96z - 0.42z^2 + 0.04z^3 - 0.002z^4 + 0.000033z^5 \tag{7c}$$
$$\text{Franciscan complex at depth of } 0.05-9 \text{ km}$$

$$V_P = 2.5 + 2.93z - 0.82z^2 + 0.102z^3 - 0.006z^4 + 0.0002z^5 \tag{7d}$$
$$\text{Granitic rocks at depth of } 0.05-4 \text{ km,}$$

where V_P is in the unit of km/s and z is depth below the ground surface in the unit of km. All equations in Eqs. (7a, 7b, 7c, 7d) are shown in Fig. 2 where the datasets of measurement are not presented. According to Eqs. (7a, 7b, 7c, 7d), it can be found that for granitic rocks $V_P = 2500$ m/s at zero depth, and $V_P = 5800$ m/s at 2000 m depth. The latter is 2.3 times greater than the former. For Great Valley rocks, $V_P = 2750$ m/s at zero depth, and $V_P = 3690$ m/s at 2000 m depth. The latter is 1.4 times greater than the former. Evidently, the higher P-wave velocities at 2000 m depth result in larger characteristic impedances at 2000 m depth than the ones at 0 m depth, even though it is assumed that the density is kept as constant.

Analytical results indicated that S-wave velocity increases with depth, too (Brocher 2008). Since the measured S-velocities were only from shallow depths (Brocher 2008), the equations based on S-wave measurements, similar to Eqs. (7a, 7b, 7c, 7d), are lacking for large depths up to kilometers.

3.3 Variation of Porosity and Poisson Ratio with Depth

In addition to density and sonic velocities, porosity and Poisson's ratio also vary with the depth below the ground surface. For example, the porosities of sandstone, shale, limestone, and dolomite decrease with increasing depth

Fig. 2 P-wave velocity vs depth (based on Eq. (7a, 7b, 7c, 7d) originating from Brocher 2008)
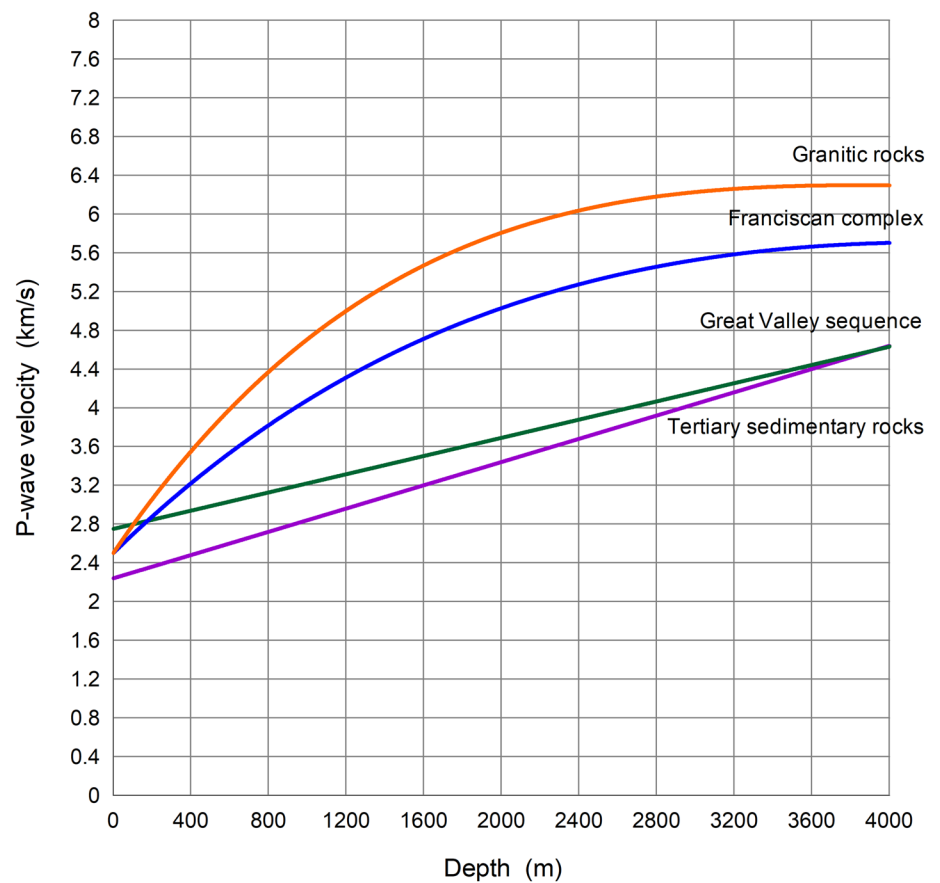
according to summarized measurement data by Schön (2015). Similarly, total porosities of sedimentary rocks decrease with increasing depth according to laboratory measurements of over 4000 samples of conventional cores from the Los Angeles and Ventura basins of California, other scattered localities in the United States, and the Po basin of Italy (McCulloh 1967). Contrary to total porosity, Poisson's ratio increases with increasing depth according to the measurements by Eaton (1969). The decrease in porosities and increase in Poisson's ratios of rocks with increasing depth are reasonable, since overburden stress or vertical stress of rocks increases with increasing depth, on the basis of both theoretical analysis (e.g., Williamson and Adams 1923) and measurements (e.g., Eaton 1969; Brown and Hoek 1978). In particular, the decrease in porosity with increasing depth can explain why density and seismic wave velocities increase with increasing depth to a certain extent.

Schön (2015), based on measured data from Dortman (1976), presented a correlation between P-wave velocity V_P and density ρ for magmatic and metamorphic rocks including granite, gneiss (biotitic, amphibolitic), gneiss (garnet biotitic), amphibole, gneiss (amphibolitic), granulite, diorite, gabbro-norite, and ultrabasite. This relation is

$$V_P = 2.76\rho - 0.98, \tag{8}$$

where the density is in 10^3 kg/m^3 and the velocity is in km/s. This empirical relation indicates that the P-wave velocity increases with increasing density of rock, and vice versa.

Note also for many rocks, both P- and S-wave velocity increase with increasing confining pressure in the range of 0–50 MPa after which the increase in the P-wave velocity is very small and slow, according to test data (Schön 2015). However, such relations depend on the rock. For instance, the P- and S-wave velocities of granite and sandstone increase rapidly with increasing pressure, but those of shale increase slowly with increasing pressure (Schön 2015).

In brief, it can be concluded that the densities of the sedimentary rock masses investigated significantly increase with increasing depth, while the densities of the metamorphic rocks measured do not markedly increase with increasing depth. The P-wave velocities of various rock masses mentioned above increase with increasing depth up to several kilometers. The S-wave velocity increases with increasing depth, too, but the measured results for S-waves are limited to a shallow depth.

4 Relation Between Characteristic Impedance and Strengths, Fracture Toughness, Young's Modulus, and Poisson's Ratio of Intact Rock

Based on a great number of experimental data on various mechanical properties of intact rocks in the literature, six empirical equations between the characteristic impedance and mechanical properties of rock are established (Zhang et al. 2020a). These equations can be divided into linear relations and nonlinear ones, as follows.

4.1 Linear Relations Between Characteristic Impedance and Strengths as Well as Poisson's Ratio

It has been found that uniaxial compressive strength σ_c, tensile strength σ_t, shear strength σ_s, and Poisson's ratio ν have linear relations with the characteristic impedance of intact rock (Zhang et al. 2020a). These linear relations based on the data regression analysis are shown in Fig. 3a in which all dataset points are not shown but the R^2 and the number of datasets for each relation is indicated. The R^2 values varies in a range of 0.80–0.97. Notice that most of the tested rocks show a linear relation between their characteristic impedances and their Poisson's ratios, but the sandstone does not follow the linear relation (Zhang et al. 2020a). Regarding this issue, a further investigation with more measurement data is needed.
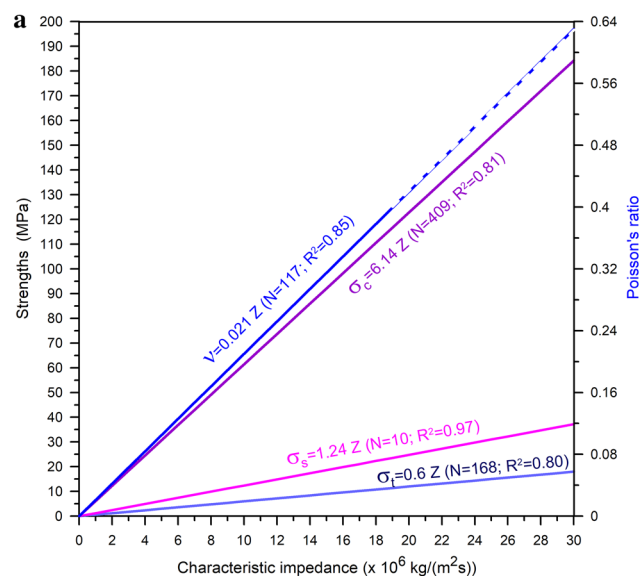
4.2 Nonlinear Relations Between Characteristic Impedance and Fracture Toughness and Young's Modulus

It has been found that mode I fracture toughness K_{Ic} and Young's modulus E have nonlinear relations with the characteristic impedance of intact rock (Zhang et al. 2020a). These nonlinear relations based on the data regression analysis are shown in Fig. 3b in which all dataset points are not shown but the R^2 and the number of datasets for each relation are shown. Clearly, mode I fracture toughness and Young's modulus increase with increasing characteristic impedance faster than the three strengths and Poisson's ratio of intact rock.

The results in Fig. 3 indicate that the characteristic impedance can represent the main mechanical and material properties such as three strengths, mode I fracture toughness, Young's modulus, and Poisson's ratio of intact rock. In other words, characteristic impedance can be considered as a comprehensive property of intact rock. In this sense, characteristic impedance can be used to classify intact rocks.

5 Relation Between Characteristic Impedance and Intact-Rock Bursts

Rock burst is a spontaneous and violent rock failure that can occur in underground mines, tunnels, and other underground openings. To evaluate rock burst proneness, many

Fig. 3 Relations between characteristic impedance and six mechanical properties of intact rock (based on the empirical equations in Zhang et al. 2020a). **a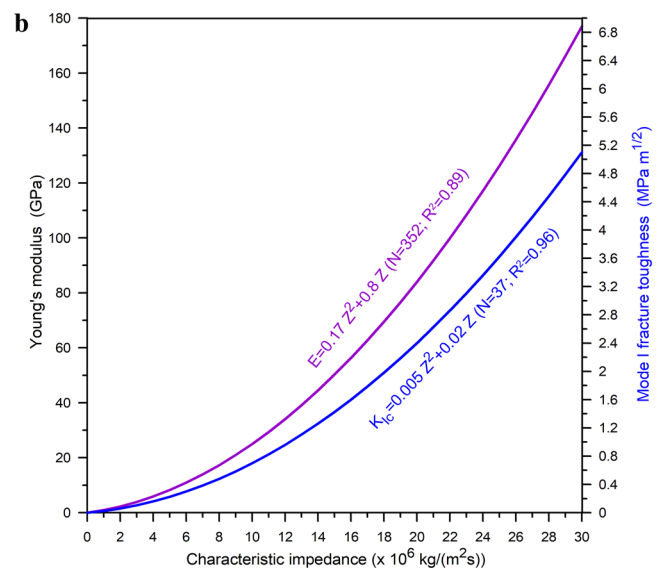** Uniaxial compressive strength, tensile strength, shear strength, and Poisson's ratio; **b** Young's modulus and mode I fracture toughness. N means the number of datasets. The data points are not shown

criteria have been proposed, as reviewed by Zhou et al. (2018) and Gong et al. (2020). Among 20 criteria of rock burst proneness reviewed by Gong et al. (2020), 12 criteria are energy-related and the rest are stress- or strain-related. For example, the method by Cook et al. (1966) uses energy release rate, and the burst-potential index by Mitri et al. (1999) employs strain energy storage rate.

Laboratory experiments using small intact rock specimens are often employed to study rock bursts. Here, the laboratory experiment results from 14 different rocks by Gong et al. (2020) are used to investigate the relation between characteristic impedance and rock bursts. In their study, the uniaxial compressive test and Brazilian test of each intact rock were carried out under static loading conditions. Table 1 shows the measured average density and P-wave velocity of each rock. Based on the measured density and P-wave velocity, the characteristic impedance of each rock can be determined. In Table 1, the rocks having strong burst phenomenon during laboratory experiments are noted by "Yes" in the last column, while those without strong burst phenomenon marked with "No". The characteristic impedance values of all 14 rocks are also shown in both Fig. 4 and Table 1, indicating that among 6 rocks having strong burst phenomenon, 5 rocks have a characteristic impedance equal to or larger than 10.8 (10^6 kg/m^{2}s). This means that the intact-rock bursts are dependent on the characteristic impedance of the rock to a great extent. In other words, strong rock bursts happen mostly in the rocks with large characteristic impedance.

6 Relation Between Characteristic Impedance and Rock Bursts in Diversion Tunnel

In the diversion tunnel excavated by drill and blast method, with a length of 8500 m, a diameter of 8.4 m, and a overburden of 100–1690 m, of the Jiangbian hydropower station in China, a total of 20 cross sections were selected to perform rock burst study (Zhang 2011). Among the 20 sections, rock bursts happened in 14 sections, while rock burst did not occur in 6 sections. From all sections, rock samples were taken to determine their mechanical and physical properties in the laboratory. The results are shown in Table 2 that includes the cross section number, rock type and weathering condition, depth, uniaxial compression strength, Young's modulus, density, and P-wave velocity of each section. In addition, Table 2 shows the characteristic impedance of each section and indicates whether rock burst occurred or not.

Based on Table 2, the characteristic impedances and depths of all sections are shown by bars and circles, respectively, in Fig. 5, indicating that among 14 sections with an impedance larger than 12.2×10^6 kg/m^{2}s, 13 sections had rock bursts, while among 6 sections with an impedance lower than 12.2×10^6 kg/m^{2}s, 5 sections did not have rock bursts. This result indicates that 12.2×10^6 kg/m^{2}s can be taken as the threshold characteristic impedance of rock burst in the tunnel, i.e., when the impedance is larger than this threshold impedance, rock burst likely occurs.

Figure 5 shows that rock burst has a certain relation with the depth. Among 6 sections having no rock burst, 4 sections have a depth smaller than 400 m, while 2 sections have a depth larger than 1000 m. Among 14 sections having rock burst, 12 sections have a depth greater than 600 m, while

Table 1 Characteristic impedance of 14 rocks (based on Gong et al. 2020)

Rock	Density (g/cm^3)	P-wave velocity (m/s)	Characteristic impedance (10^6 kg/m^{2}s)	Indication of strong burst in experiment
Limestone	2.69	6137	16.5	**Yes**
Fine granite	2.80	5419	15.2	**Yes**
Slate	2.75	4753	13.1	**Yes**
Marble	2.69	4272	11.5	No
Yueyang granite	2.60	4155	10.8	**Yes**
Qingshan granite	2.64	4082	10.8	**Yes**
Red granite	2.60	4122	10.7	No
White marble	2.70	3962	10.7	No
Yellow sandstone	2.57	3964	10.2	No
Black sandstone	2.59	3733	9.7	No
Yellow rust granite	2.58	3451	8.9	No
Yellow granite	2.58	3336	8.6	**Yes**
Green sandstone	2.41	3022	7.3	No
Red sandstone	2.43	2824	6.9	No

Fig. 4 Characteristic impedances of 14 rocks tested by Gong et al. (2020) in laboratory

B: strong burst occurred
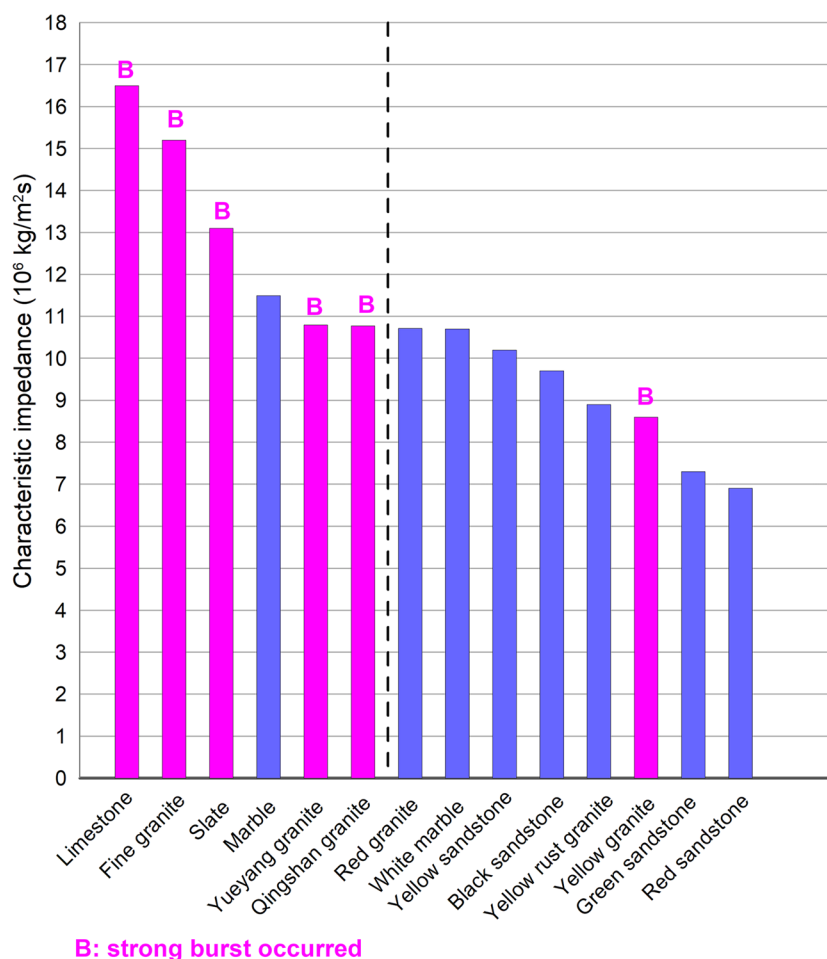
only 2 sections have a depth smaller than 400 m. In brief, most rock bursts happened in large depths, while only a few occurred in small ones.

7 Relation Between Characteristic Impedance and Rock Bursts in Mines

7.1 Rock Bursts Dependent on Mining Location, Rock Mass, and Depth

During several-year mining production in Kiruna mine, seismic events in three blocks were investigated (Nordström et al. 2017). The result indicated that more than 1000 seismic events per day were recorded in the whole mine during that time. It was found that one block numbered Block 33/34 was burst-prone where largest and most events occurred, but two other blocks were not burst-prone. In Malmberget mine, some ore bodies were burst-prone but others not. Even in a long and narrow ore body named Parta, one part was burst-prone but the other not. In Zhazixi antimony mine, strong rock bursts occurred often in massive stibnite but not

in other rock masses (Ma et al. 2018). These three examples indicate that rock bursts are dependent on the rock mass and mining location.

It has been reported that with increasing mining depth, both number and magnitude of rock bursts increase in many mines (e.g., Brauner 1994; He and Qian 2010; Nordström et al. 2017; Ma et al. 2018; Cai et al. 2020; Jiang et al. 2020). In general, as mining operations reach a certain depth such as several hundred meters, seismic events and rock bursts start to occur. For example, in Kiruna mine when the mining depth increased to 670 m below the ground surface substantial problems with seismicity and rock bursts started (Dineva and Boskovic 2017), and the seismic activity increased as mining advanced deeper (Nordström et al. 2017). In Malmberget mine, the first rock burst happened at an iron orebody at the depth 615 m (Stålnacke 2022). In Zhazixi antimony mine, rock burst first appeared when mining depth reached 560 m below the ground surface. When mining to 605 m depth, more and stronger rock bursts occurred (Ma et al. 2018). These examples indicate that when the mining activity reached a certain depth, rock bursts may happen.

Table 2 Mechanical and physical properties of rocks at 20 cross sections of the diversion tunnel of the Jiangbian hydropower station (based on the data of Zhang 2011)

Cross section number	Rock	Weathering	Depth (m)	UCS (MPa)	Young's modulus GPa	Density (kg/m³)	P-wave velocity (m/s)	Rock burst	Impedance (10⁶ kg/m²s)
13	Biotite quartz schist	Nearly intact and lightly weathered	1374	84	16.7	2700	4110	No	11.1
2	Biotite granite	Intact, lightly or not weathered	275	106	19.4	2640	4262	No	11.3
12	Biotite quartz schist	Nearly intact and lightly weathered	1184	89	16.9	2700	4227	No	11.4
11	Biotite quartz schist	Nearly intact and lightly weathered	1205	107	20.7	2700	4303	**Yes**	11.6
3	Biotite granite	Intact, lightly or not weathered	187	118	20.7	2640	4493	No	11.9
1	Biotite granite	Intact, lightly or not weathered	174	114	22.7	2640	4530	No	12.0
8	Biotite granite	Intact, lightly or not weathered	693	135	24.5	2640	4640	**Yes**	12.2
10	Biotite quartz schist	Nearly intact and lightly weathered	1107	114	23.8	2700	4524	**Yes**	12.2
17	Biotite quartz schist	Nearly intact and lightly weathered	920	124	24.1	2700	4524	**Yes**	12.2
14	Biotite quartz schist	Nearly intact and lightly weathered	1690	117	19.3	2700	4631	**Yes**	12.5
15	Biotite quartz schist	Nearly intact and lightly weathered	1606	128	23.7	2700	4666	**Yes**	12.6
5	Biotite granite	Intact, lightly or not weathered	215	139	25.3	2640	4818	No	12.7
19	Biotite quartz schist	Nearly intact and lightly weathered	773	122	24.9	2700	4769	**Yes**	12.9
4	Biotite granite	Intact, lightly or not weathered	267	148	24.9	2640	4922	**Yes**	13.0
6	Biotite granite	Intact, lightly or not weathered	272	141	27.4	2640	4922	**Yes**	13.0
20	Biotite quartz schist	Nearly intact and lightly weathered	644	164	28.5	2700	4870	**Yes**	13.1
16	Biotite quartz schist	Nearly intact and lightly weathered	1220	140	28.3	2700	4936	**Yes**	13.3
9	Biotite granite	Intact, lightly or not weathered	970	161	30.9	2640	5090	**Yes**	13.4
7	Biotite granite	Intact, lightly or not weathered	645	152	26.3	2640	5090	**Yes**	13.4
18	Biotite quartz schist	Nearly intact and lightly weathered	785	186	31.5	2700	5130	**Yes**	13.9

Fig. 5 Characteristic impedances (vertical axis in the left) and depths (vertical axis in the right) of 20 cross sections of the diversion tunnel in the Jiangbian hydropower station (based on the data from Zhang 2011)
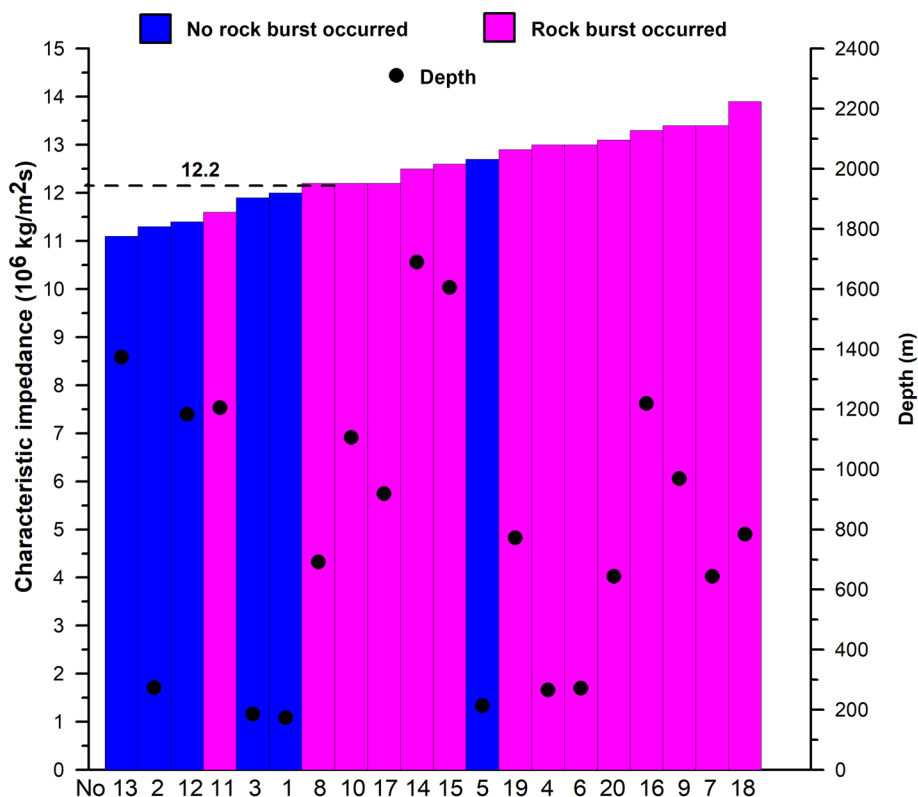
Based on the above description, the depth in which the first rock burst occurs can be defined as the threshold depth of rock bursts, and the characteristic impedance either Z_P or Z_S at this depth is defined as critical characteristic impedance either Z_{cP} or Z_{cS}. Rock bursts occurred in three mines—Kiruna, Malmberget and Zhazixi—demonstrate that this threshold depth exists. The threshold depths of three mines are listed in Table 3. The determination of the critical characteristic impedance Z_{cP} in Table 3 will be described in the next section.

7.2 Rock Bursts Related to Characteristic Impedance

(1) Zhazixi Antimony Mine

As mentioned earlier, strong rock bursts occurred often in massive stibnite but not in other rock masses in Zhazixi antimony mine. Based on the measured Young's modulus, density and Poisson ratio of each rock/ore from the mine

(Ma et al. 2018), the P-wave velocity, and characteristic impedance of each rock/ore mass can be calculated and the results are shown in Table 4. Obviously, the massive stibnite has the largest characteristic impedance up to 15.9 (10^6 kg/m^{2}s), compared with other rock masses in the mine (Ma et al. 2018).

(2) Sanhejian Coal Mine

The Sanhejian coal mine in Xuzhou, China is a rock burst-prone mine (He et al. 2017). A rock burst which occurred in an area with a high P-wave velocity up to 5.5–6.0 km/s on January 30, 2015. According to He et al. (2017), most other mining areas had P-wave velocities equal to or lower than 5.5 km/s, implying that the characteristic impedance of that area might be larger than the characteristic impedances of other areas.

(3) Malmberget Mine and Kiruna Mine

The density and P-wave velocity of iron ore mass in Malmberget mine are about 4800 kg/m^3 and 5100 m/s, respectively (Zhang 2014). The density of the iron ore mass

Table 3 Threshold depth and critical characteristic impedance of rock burst from three mines

Mine	Rock/ore mass	Critical depth (m)	Critical characteristic impedance Z_P (10^6 kg/m^{2}s)	References
Kiruna	Iron ore	670	24.5	Dineva and Boskovic (2017)
Malmberget	Iron ore	615	24.0	Stålnacke (2022)
Zhazixi	Antimony ore	560	15.9	Ma et al. (2018)

Table 4 Characteristic impedances of rocks in Zhazixi antimony mine (the P-wave velocity was calculated using the measured Young's modulus, density and Poisson ratio in Ma et al. (2018))

Lithology	Density (kg/m^3)	P-wave velocity (m/s)	Impedance Z_P (10^6 kg/m^{2}s)	Occurrence of strong rock-burst
Slate	2810	2666	7.5	No
Quartz sandstone	2750	3091	8.5	No
Tuffaceous slate	2900	3535	10.3	No
Tuffaceous sandstone	2700	4036	10.9	No
Disseminated stibnite	3120	4072	12.7	No
Massive stibnite	3840	4132	15.9	**Yes**

in Kiruna mine is 4700 kg/m^3 (Malmgren and Nordlund 2006) and the P-wave velocity of the ore mass is close to that of the ore mass in Malmberget mine, i.e., 5100 m/s. Furthermore, it is assumed that those densities and P-wave velocities are close to the corresponding values of the first or earliest rock bursts in the two mines. Then, it can be obtained that the characteristic impedance $Z_P = 24.0 (10^6$ kg/m^{2}s) for the Kiruna ore mass, and $Z_P = 24.5 (10^6$ kg/m^{2}s) for the Malmberget ore mass when the first rock burst happened. As mentioned in Sect. 7.1, in both Kiruna and Malmberget mine, seismic events and rock bursts increase with increasing mining depth. For example, the largest seismic event in Kiruna mine occurred on May 18, 2020 reached up to 4.9 Richter's scale (Zhang et al. 2021). This seismic event and corresponding rock burst had made mining production stopped for months in part of the mine.

In summary, the above description indicates that rock bursts are dependent on the depth below the ground surface and the rock (ore) mass. Since the depth and rock (ore) mass are both related to the characteristic impedance of rock, it can be inferred that rock bursts are related with the characteristic impedance of rock mass.

7.3 Critical Characteristic Impedances in Underground Mines

7.3.1 Zhazixi Antimony Mine

As mentioned in Sect. 7.2, strong rockbursts happened often in massive stibnite but not in other rock masses in Zhazixi antimony mine (Ma et al. 2018). As shown in Table 4, the characteristic impedance Z_P of the massive stibnite is 15.9 (10^6 kg/m^{2}s), while the characteristic impedances of the other rock masses in the mine are smaller than 15.9 (10^6 kg/m^{2}s). Thus, it is assumed that $Z_{cP} = 15.9 (10^6$ kg/m^{2}s). Accordingly, it can be inferred that if $Z_P \geq 15.9 (10^6$ kg/m^{2}s) in a place in the Zhazixi mine, the place will be burst-prone.

7.3.2 Sanhejian Coal Mine

In the Sanhejian coal mine, the first rockburst happened in 1991, but the detailed data of the first burst were not reported (He et al. 2017). However, the rockburst which occurred on January 31, 2015 was described in detail by He et al. This rockburst occurred in the coal with a high P-wave velocity up to 5.5–6.0 km/s and a density of 1350 kg/m^3. Using the lower bound of the P-wave velocity (i.e., 5.5 km/s) and the density of the coal, it can be determined that the characteristic impedance Z_P of the coal is equal to 7.4 (10^6 kg/m^{2}s). Since the data of the characteristic impedance of the first rockburst are not available, it is assumed that $Z_{cP} = 7.4$ (10^6 kg/m^{2}s) for the Sanheijian mine.

7.3.3 Kiruna and Malmberget Mine

Based on the description in Sect. 7.2, it can be determined that the critical characteristic impedance $Z_{cP} = 24.0 (10^6$ kg/m^{2}s) for the Kiruna ore mass, and $Z_{cP} = 24.5 (10^6$ kg/m^{2}s) for the Malmberget ore mass.

In summary, the critical characteristic impedance of rockburst is different from one mine to another. Figure 6 shows the critical characteristic impedances of four mines mentioned above. As a comparison, the critical characteristic impedances of the diversion tunnel discussed in Sect. 6 and the laboratory rock specimens from Gong et al. (2020) are shown in Fig. 6, too. Clearly, the critical characteristic impedances of the two iron mines are the highest, the critical characteristic impedance of the coal mine is the minimum, and the critical characteristic impedances of the antimony mine, the laboratory specimens, and the tunnel rock are in the between.

7.4 P-Wave Velocity and Seismic Events

Previous studies indicated that the zones with high P-wave velocity were correlated with large seismic events (Lurka 2008; Bańka and Jaworski 2010; Dou et al. 2012, 2014; Cai et al. 2015). In addition, Cai et al. (2015) showed that the maximum P-wave velocity of the coal seam being mined,

Fig. 6 Critical characteristic impedances Z_{cP} of four mines, one tunnel, and laboratory specimens
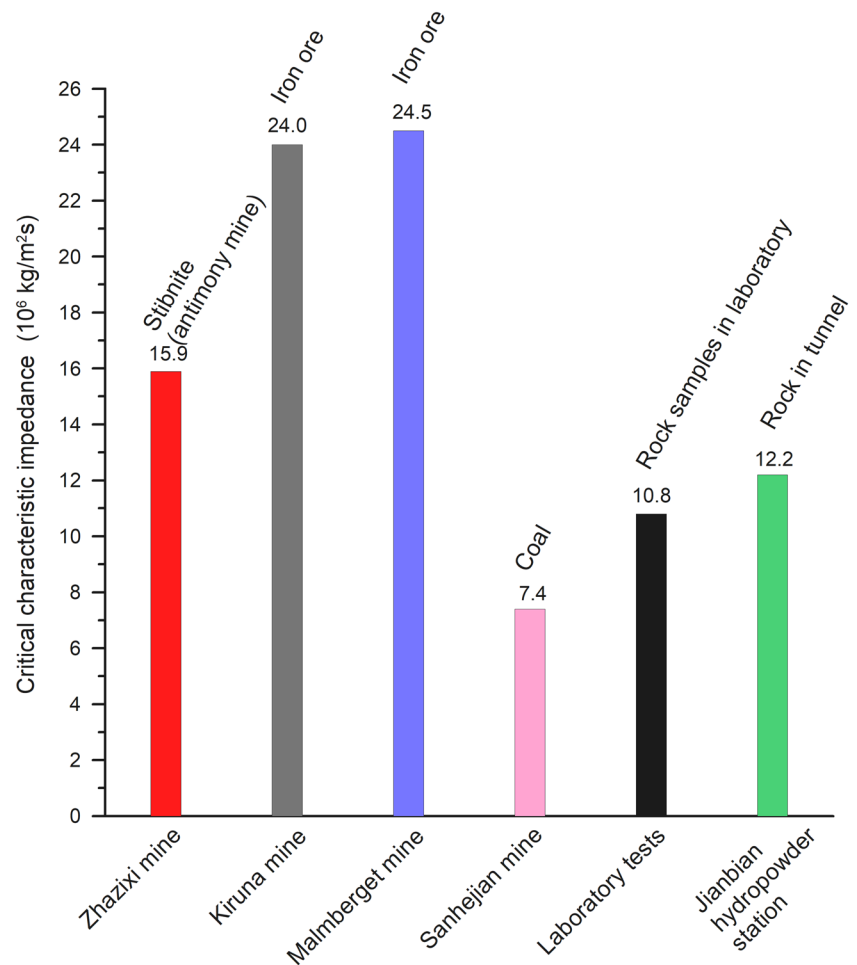
where most seismic events happened, was up to over 5000 m/s, but the P-wave velocities of other coal seams were mostly below 3000 m/s, implying that the P-wave velocity became higher in the coal mass when seismic events occurred.

7.5 Varying P-Wave Velocity of Rock

7.5.1 Laboratory Measurement Result

Laboratory experiments of different rock samples show that seismic velocity increases as applied stress rises (Scott et al. 1994; Khaksar et al. 1999; He et al. 2018).

During cyclic loading to coal and sandstone samples, Jia et al. (2019) recorded P-wave velocity throughout the test and found that P-wave velocity varied in the whole cyclic loading process, consisting of three phases: (I) compaction; (II) crack initiation; (III) strain acceleration. They observed that in the compaction phase (I), the deformation was mostly elastic with few new crack formations, and the stress enabled the pre-existing cracks to close, making the sample volume to shrink and the P-wave velocity increased by about 9%

for coal and 6% for sandstone samples, compared with the initial value (before compression). In the crack initiation phase (II), at around 30% of peak stress, the wave velocity reached its maximum value, and then fluctuated around this value until about 50% of its strength. Then, from the middle of phase (II), wave velocity decreased slowly because of the micro-crack formation. Finally, at the beginning of the phase (III), an abrupt decrease occurred of wave velocity of ~7–9% coinciding with accelerated deformation and surface macro-crack formation.

Lin and Wang (1980) determined the P-wave velocities of six rocks under different confining pressures and at various temperatures in laboratory. Their experimental results are summarized in Fig. 7. Based on the results, the following conclusions can be drawn: (1) the P-wave velocities of all six rocks increase with increasing confining pressure in the range of 0–700 MPa and at 20 oC temperature. (2) In the pressure range of 0–200 MPa and at 20 oC temperature, the P-wave velocities of all rocks increase rapidly with increasing pressure presumably due to crack closure, and after 200 MPa pressure, the P-wave velocities increase slowly with increasing pressure. (3) In the pressure range of

Fig. 7 P-wave velocity vs confining pressure (based on measurement results shown in Figs. 5–10 of Lin and Wang 1980)
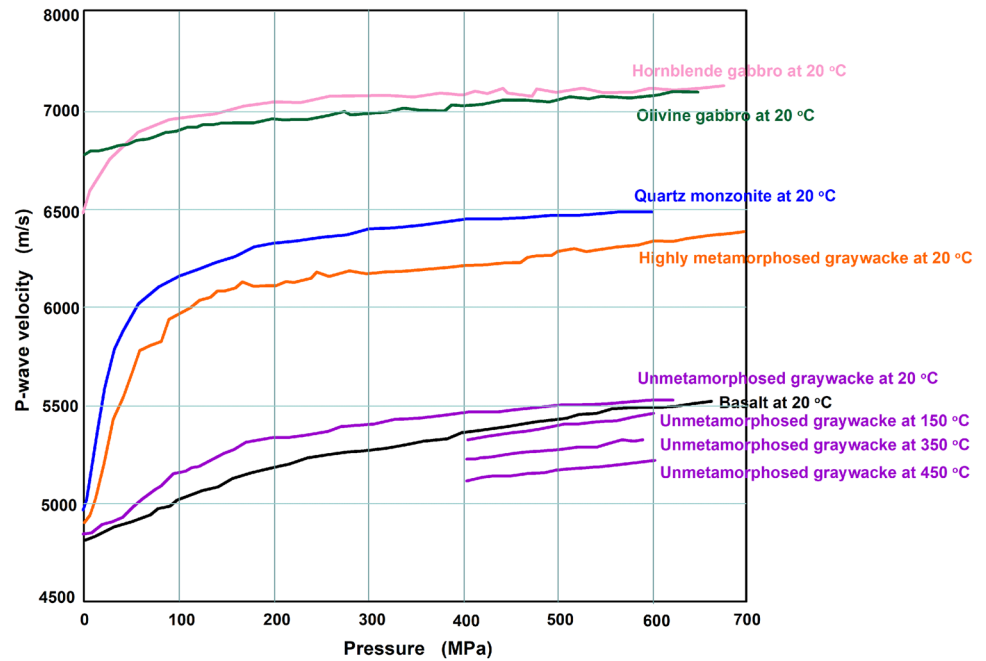
0–100 MPa and at 20 °C temperature, the P-wave velocities of most rocks increase with increasing pressure at maximum speed. Note that this pressure range covers the insitu stresses of most present underground mines and other deep constructions. (4) The effect of confining pressure on P-wave velocity depends on rock type. For instance, with an increasing confining pressure and at 20 °C temperature, quartz monzonite and highly metamorphosed graywacke have maximum increase in their P-wave velocities, olivine gabbro has minimum increase in its P-wave velocity, and unmetamorphosed graywacke, balsal, and hornblende gabbro have an increase in the between. (5) At a specific high temperature, the P-wave velocity of each rock (only the result of unmetamorphosed graywacke is shown in Fig. 6) increases linearly with increasing confining pressure. (6) At a specific pressure, the P-wave velocity of each rock is greater at lower temperature than at higher temperature.

7.5.2 Field Result

Field scale analysis demonstrates that areas with higher velocity generally correspond to higher stress concentrations (Kerr 2011; Westman 1993). Hosseini et al. (2012, 2013), using passive seismic velocity tomography to reveal the stress state around a longwall mining panel, found that high-velocity regions matched regions under high-abutment stress and that the stressed zones moved as the working face was advanced. However, there are different findings from other mines. For instance, using passive seismic tomography, Afrouz et al. (2021) analysed three seismic events in a mine and found that the P-wave velocity did not increase in

the vicinity of the hypocenter for any of the three events. For two of the events, the velocity deceased in the week prior to the event (by 2.1% and 0.8%), and for the third event, the velocity was essentially unchanged from the week prior. Afrouz et al. (2021) explained that a potential reason was that new fractures might be developing within the highly stressed rock mass, resulting in either no increased velocity or a reduction in velocity at the hypocenter prior to the seismic event. In addition, they reported that the three seismic events might be due to the different failure mechanisms, since Events 1 and 3 occurred suddenly followed by several minor events, while Event 2 triggered fewer subsequent minor events but was followed by a major event 17 days later. Therefore, it is necessary to investigate the relation between the seismic wave velocity and significant seismic events further at more mines, since such a relation is helpful for predicting seismic events. For example, based on the variation of P-wave velocity and other factors such as released energy ratio and shear component of the moment tensor, Feng et al. (2017) introduced a warning method for rockburst monitoring systems in mines to first characterize the type of failure and then estimate the probability of failure.

8 Relation Between Characteristic Impedance and Rock Drillability

Rock drillability is often determined with a sophisticated instrumentation in laboratory. Many studies have indicated that rock drillability has a certain relation with some of rock properties such as uniaxial compressive strength,

P-wave velocity, density, porosity, Brazilian tensile strength, point load strength, and Schmidt hardness of rock (e.g., Howarth et al. 1986; Kahraman et al. 2003; Taheri et al. 2016; Bilim and Karakaya 2021).
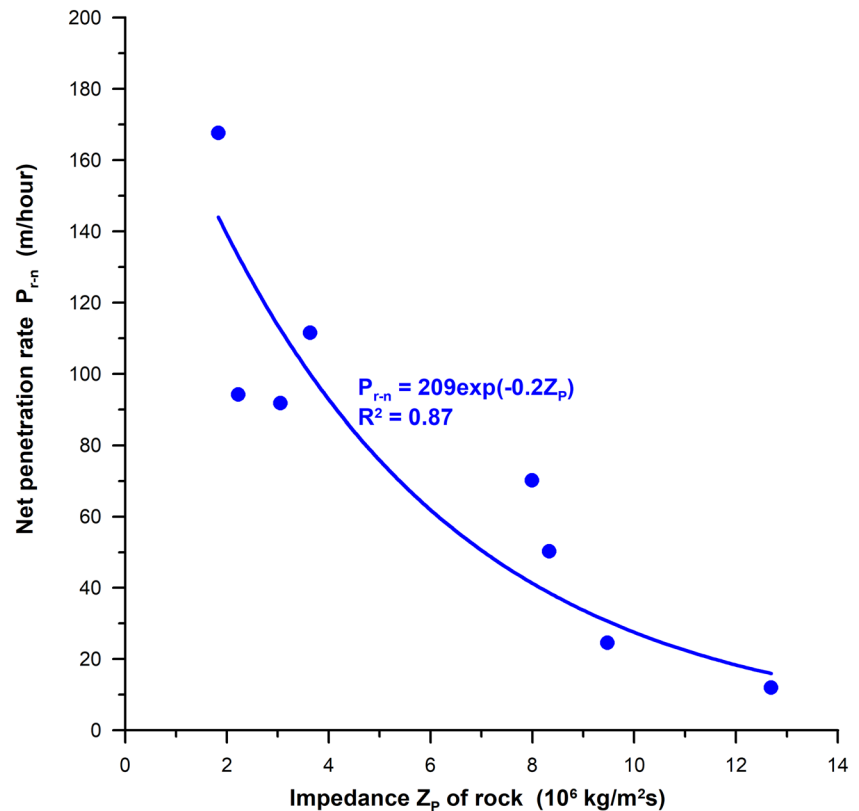
The above description indicates that it is possible to predict the drillability of a rock using its physical and mechanical properties. Unfortunately, most mechanical properties of rock can be determined only in laboratory using small rock samples. Accordingly, these mechanical properties cannot be used directly to evaluate rock mass containing geological structures such as faults and joints.

A preliminary investigation (Zhang and Hou 2022) found that the characteristic impedance Z of rock mass has a good relation with the net penetration rate P_r of rotary drilling, based on the field measurements in several rock formations by Kahraman et al. (2000). This relation is shown in Fig. 8 and in Eq. (9)

$$P_r = a \exp(b Z_P), \tag{9}$$

where a and b are constants from the regression analysis. Figure 8 indicates that $a = 209$, and $b = -0.2$, based on the data of Kahraman et al. (2000). Obviously, the characteristic impedance Z_P is well related to the net penetration rate according to the field drilling results.

9 Applications of Characteristic Impedance

9.1 Current Applications

When an elastic wave propagates from one material to another, the ratio of characteristic impedances of the two materials will decide how much of the wave is reflected (or transmitted) and whether the reflected wave is tensile wave or compressive wave, according to elastic stress wave theory (e.g., Kolsky 1963; Wang 2007; Zhang 2016). This principle is often used in the study of percussive rock drilling and the development of drill tool, since drill rod/pipe, impact hammer, drill bit, and the rock beneath the bit are all loaded by stress waves during drilling. Moreover, this principle was applied to develop a method for reducing the ground vibrations caused by rock blasting (Zhang and Naarttijärvi 2005; Zhang 2012, 2016). In the method, a new fractured zone was created by blasting itself between the ore mass and the rock mass by making full use of the different impedances of the three materials (original ore mass, original waste rock mass, and the fractured ore mass by blasting). Using the method, the vibrations in the Malmberget mine were largely reduced (Zhang 2012, 2016).

For a specific mine or a rock project, the explosive to be used should match the rock mass to be blasted in rock blasting (Nicholls and Duvall 1963), and it is better that the

Fig. 8 Net penetration rate vs characteristic impedance (based on data from Kahraman et al. 2000)

$$P_{r-n} = 209\exp(-0.2Z_P)$$
$$R^2 = 0.87$$

detonation velocity of the explosive is equal to or greater than the P-wave velocity of the rock (Zhang 2016). Otherwise, if the detonation velocity is smaller than the P-wave velocity, the P-wave will arrive to the undetonated explosive charge earlier than the detonation wave, resulting in that the P-wave will press the explosive and possibly cause dead pressing to it, i.e., the pressed explosive will not be fired. Such dead pressing did happen (Farnfield and Williams 2011; Mencacci and Farnfield 2003). When this dead pressing happens, the explosive as well as the detonators in it will fail. In addition, the characteristic impedances of both the explosive and the rock play an important role in blasting, since they influence the propagation of the detonation wave from the blast hole to the rock. Furthermore, when the detonation wave travels from detonated explosive to the stemming, the ratio of the impedance of the detonation product (high-pressure and high-temperature gases) to the impedance of the stemming effects the propagation of shock and stress waves and the ejection of gas and stemming material (Zhang 2016). Note that in some mines or sites, the P-wave velocity of a rock mass may be higher than the maximum detonation velocity of current commercial explosives such as emulsion and ANFO. In such a case, it is difficult to achieve a satisfied match between the explosive and the rock mass, but it is better to increase the detonation velocity as much as possible, so that the difference between the detonation velocity and the P-wave velocity can be reduced to a minimum value.

Characteristic impedance has other applications. For example, it was employed as a rock property to determine the crushed zone surrounding the blasthole (Kou and Rustan 1993); it was used to study the energy transferred to the rock (Cai et al. 2010; Nicholls 1962). In blasting experiments using cement-mortar and granite, Bhandari (1979) found that the granite which had higher impedance produced greater amount of fine fragments, and in all the tests, larger amount of new surfaces were created. In a field investigation Cai et al. (2010) found that greater elastic wave energy was produced when the ratio of the impedance of explosive to that of the rock varied from 1.8 to 2.0; however, this energy decreased when the impedance ratio was too high. Early impedance-coupling tests by Nicholls (1962) indicated that the maximum seismic amplitude or energy was generated in a rock by the detonation of explosive as the charge diameter equalled the drill hole diameter and as the characteristic impedance of the explosive equalled that of the rock. This finding is reasonable, since there was no wave reflection when both impedances were equal.

Characteristic impedance can be used in exploration of natural resources. In geophysics seismic traces are converted into pseudoreflection-coefficient time series and then into characteristic impedance by the inversion of the time series. Such pseudologs were roughly equivalent to logs recorded in wells drilled at every seismic trace location and they produced important information concerning the nature of the rock and variations in lithology (Becquey et al. 1979). Such information can be used to estimate mineral or other natural resources such as hydrocarbon reserves.

9.2 Potential Applications

9.2.1 Possibility of Rock Mass Evaluation Using Characteristic Impedance

Characteristic impedance was suggested to evaluate the quality of a rock mass and classify it, because the impedance could well represent the actual state of the rock mass such as geo-structures like joints, faults, and bedding as well as mineral components (Zhang 2016). Suppose that there are two different rock masses, one is similar to an aluminium with a P-wave velocity of over 6000 m/s and the other similar to a steel with a P-wave velocity of over 5500 m/s. If only P-wave velocity is used to evaluate these two masses, it can be found they are similar, i.e., there is a small discrepancy between them. However, if their densities are considered together with their P-wave velocities and it can be found that their impedances are much different from each other since the density of common aluminium is about 2700 kg/m^3, while that of ordinary steel around 7800 kg/m^3. In other words, the impedance of the steel is about 2.6 times of the impedance of the aluminium. This large difference in their impedances can explain why the steel is stronger than the aluminium in common sense, even though their P-wave velocities are quite close to each other. This example indicates that only P-wave velocity is not enough to evaluate and classify rock masses, but characteristic impedance may be taken as a comprehensive index to evaluate and classify rock masses. Take the three ore masses in Fig. 6 as example, we can see that the iron ore has the maximum impedance, the coal does the minimum impedance, and the stibnite has the impedance in the between. This is consistent with our common sense: iron ore is the strongest, coal is the weakest, and stibnite in the between. In brief, it is possible to use impedance to evaluate and classify rock masses.

9.2.2 Possibility of Evaluating Rock Burst Proneness Using Characteristic Impedance

According to the definition of rock burst given by Gibowicz and Kijko (1994), as mentioned in Sect. 1, rock burst must satisfy a prerequisite that a rock mass has at least one free surface nearby (or an open fracture inside the rock mass) or the rock mass is under one- or two-dimensional loading conditions. If this prerequisite is met and the following inequation is satisfied, it is possible that a rock burst may happen:

$$P_{rb} = \frac{Z_P}{Z_{cP}} = \frac{\rho V_P}{\rho_c V_{cP}} \geq 1, \tag{10}$$

where P_{rb} is the proneness of rock burst, $Z_P = \rho V_P$ is the characteristic impedance of the rock mass at a specific location in question, and $Z_{cP} = \rho_c V_{cP}$ is the characteristic impedance of the rock mass at the place where the earliest rock burst occurred in the same rock mass in the same mine or same underground openings. Here, only the characteristic impedance corresponding to the P-wave of the rock is used to judge the proneness of rock burst. If the impedance corresponding the S-wave is available, one more inequation like Eq. (10) can be used together with Eq. (10) to judge the proneness of rock burst. Notice that if a rock mass does not have any free surface nearby (or inside) or the rock mass is under three-dimensional loading condition, rock burst may not happen, even though $P_{rb} \geq 1$.

The advantages of evaluating rock burst proneness using characteristic impedance are: (1) non-destructive method can be used to determine the density and seismic wave velocity of rock mass, i.e., there is no need to take out rock samples from the field to do laboratory experiments; (2) the true characteristic impedance of rock mass can be determined in the field by seismic monitoring system and some geophysics methods; (3) the field monitoring or measurement of the characteristic impedance of rock mass can be performed online (e.g., via a seismic system and muon telescope or a geophysics system) and included in the whole online production system of a mine or a project. Considering that rock burst is dependent on multiple factors such as rock properties, stress, and deformation at concerned locations, the evaluation method of rock burst proneness using only characteristic impedance needs validation by more rock burst data. If necessary, Eq. 10 may be modified by considering other factors excluding the characteristic impedance.

Since rock bursts are generally associated with or triggered by seismic events (Simser 2019), it is interesting to investigate the relation between the proneness of seismic events and the characteristic impedance of rock mass in the future.

9.2.3 3D Model of Characteristic Impedance Distribution

As described previously, rock bursts depend on the depth, location, and rock mass including its geostructure. For example, in Kiruna and Zhazixi mines, strong rock bursts happen manly in one block or one type of rock mass but not all mining areas. Thus, a 3D model for the distribution of characteristic impedances can be established for a mine. This 3D model can be used (1) to find the regions with high rock burst proneness, so that necessary measures such as distressing method can be taken in the earliest stage to reduce or mitigate rock bursts, (2) to select most suitable explosive based on the characteristic impedance of the rock mass to be blasted, (3) to make proper rock support design, e.g., according to the rock burst proneness of the rock mass, and (4) to predict rock drillability which is to be described in the next subsection.

9.2.4 Prediction of Rock Drillability

Description in Sect. 8 shows that the characteristic impedance of rock mass is well related with the net penetration rate of rotary drilling, indicating that the penetration rate of rotary drilling can be predicted by the characteristic impedance of the rock mass. Since characteristic impedance can be determined by non-destructive methods even in the field, the prediction of drillability of rock mass using the impedance may be done more easily than other current methods for predicting drillability. However, this prediction method using Eq. (9) needs validation by more laboratory experiments and field measurements.

10 Discussion

10.1 Determination of Characteristic Impedance

To evaluate rock burst proneness in a mine or a rock mass, it is better to determine the characteristic impedance of the rock mass via field measurements. Presently, the P- and S-wave velocities in a mine or a large rock construction project can be measured using a seismic monitoring system that is widely installed in large underground mines. In small mines with no seismic monitoring system, other methods such as vibration monitors may be used to measure the wave velocities in principle. The density of rock mass can be measured by geophysics methods as used by Eaton (1969) and Brocher (2008). However, such methods are costly expensive and therefore limited for mine applications. Optimistically, a potential non-destructive method named muography may be used to determine the density of a rock mass in the field where muon telescopes or monitors can be installed permanently or flexibly (Zhang et al. 2020b; Holma et al. 2022). Since a muon telescope or monitor can be placed in a tunnel, an underground room and even a borehole, an online measurement can be realized. In addition, it is possible to estimate characteristic impedance of rocks using soft computing models (Aladejare et al. 2022).

In general, the deformation and failure of rock specimens in laboratory experiments are different from the deformation and failure of the rock mass from which the specimens are taken out, since the rock specimens used in laboratory do not have any in-situ stresses at all after the specimens are taken out from the field, as mentioned earlier. Therefore, the results from laboratory experiments on rock burst cannot

be directly applied to an engineering project dealing with rock bursts.

From the Outokumpu deep drillhole down to 2516 m, the P-wave and S-wave velocities of the rocks determined from their mineral compositions do not markedly vary with increasing depth, but both velocities measured from the core samples taken from the drillhole generally decrease with increasing depth (Gorbatsevich et al. 2011). From another deep hole named Kola superdeep borehole (SG-3) down to a depth of ~25 km, the measurement to the core samples taken from the hole *down* to 12,000 m indicates that both density and seismic velocities of rocks decrease with increasing depth when the depth is over 5 km (Gorbatsevich 2014). Such decrease in the density and the wave velocities is considered to be caused by the samples decompaction during their extraction from a great depth and lithostatic pressures and temperature release (Gorbatsevich et al. 2011; Gorbatsevich 2014). The above description shows that (1) the core samples measurement in laboratory can deliver false results if the cores are taken from deep holes where in-situ stresses as well as temperature are high, and (2) it is better to determine the characteristic impedance using the data of the density and seismic wave velocities from field measurement.

Since measured wave velocity and density may vary significantly, especially in the field, it is better to measure them multi-times, so that an average value can be obtained to determine the characteristic impedance. In addition, it is better to determine two characteristic impedances Z_P from the P-wave velocity and Z_S from the S-wave velocity.

10.2 Variation of Characteristic Impedance with Depth

In some cases or some formations of rocks such as some metamorphic and igneous rocks, neither seismic velocities nor densities of such rocks may consistently increase with increasing depth. For example, in the Outokumpu drillhole which is mentioned above and located in a formation of Palaeoproterozoic metasediments (mica gneiss/schist), the P- and S-wave velocities determined by the mineral components slightly vary with the depth, and both velocities at the depth of 1600–2229 m are somewhat higher than the ones above 1600 m (Gorbatsevich et al. 2011). In the Kola superdeep borehole down to a depth of ~25 km (Gorbatsevich 2014), both P- and S-wave velocities of the rocks in the depth of 0–12 km are 5.8–6.6 km/s and 3.1–3.9 km/s, respectively, i.e., both velocities do not vary very much with depth. The real velocity values may be influenced by several reasons such as the temperature, the pressure (in-situ stresses), and the mineral compositions of rocks as well as the crystalline restructuring of rocks owing to long-term metamorphic transformations of some minerals into others, according to Gorbatsevich (2014). In brief, the general tendency of increase in the density and seismic velocities of rock mass with increasing depth, as shown in Figs. 1 and 2, may not exist in all formations of rocks.

10.3 Variation of Characteristic Impedance Due to Damaging or Cracking

As described in Sect. 7.5.1, seismic wave velocity of laboratory rock specimens increases with increasing applied stress. This result is consistent with the field monitoring result in Sect. 7.5.2 showing that areas with higher seismic wave velocity generally correspond to higher stress concentrations. Assuming that the density of a rock mass is considered to be constant before the applied stress is increased up to a critical value at which micro-cracks start to be formed, the increasing stress will result in higher characteristic impedance of the rock mass. Consequently, an increasing characteristic impedance means that the rock mass has higher proneness of rock burst according to Eq. (10) if there is one or more free surfaces in the rock mass. It is interesting to investigate whether the increase of characteristic impedance of a rock mass can be controlled or not by changing mining planning or mining operations in the future.

The description in Sect. 7.5.1 also indicates that seismic wave velocity decreases when micro-cracks are formed, and then, an abrupt decrease in the wave velocity occurs when the deformation of the rock is accelerated and the surface macro-crack is formed. In this process, the characteristic impedance of the rock must decrease noticeably, since the density of the rock may decrease as well due to the production of both micro-cracks and macro-crack. Therefore, a decreasing characteristic impedance of a rock means that the rock has been fractured. In this sense, variation of characteristic impedance may be used to judge whether or not a rock is damaged and how much the damage is.

10.4 Prediction of Rock Burst Proneness and Drillability

Sections 9.2.2 and 9.2.4 indicate that it is possible to predict rock burst proneness and drillability using its characteristic impedance. In practice, it is simple to measure the seismic or sonic velocity of rock mass. Relatively, it is difficult to measure the onsite density of rock mass. To determine the characteristic impedance of rock mass, new technology like muography is potentially helpful, since it can be used to determine onsite density. If it is not possible to measure the onsite density of rock mass, another option is to use the density measured from small rock samples in laboratory to represent the onsite density of rock mass, but this may cause a certain error. Therefore, in the future, it is necessary to conduct as many measurements as possible of the densities of rock or rock mass so as to validate the method

for predicting rock burst proneness or drillability using the characteristic impedance of rock mass. In addition, it is good to compare the characteristic impedance method with the sonic velocity method for evaluating and classifying rock mass in the future.

11 Concluding Remarks

For an intact rock, its characteristic impedance can be considered as a comprehensive physical property, since the impedance is well correlated with the uniaxial compressive strength, tensile strength, shear strength, fracture toughness, Young modulus, and Poisson's ratio.

The bursts of intact rocks in laboratory are dependent on their characteristics impedances to a great extent, i.e., strong rock bursts happen mostly in the rocks with high characteristic impedance.

For many rock masses mentioned in this article, their densities and seismic velocities (or characteristic impedances) below the ground surface markedly increase with increasing depth, but the general tendency of increase in the densities and seismic velocities with increasing depth, may not exist in all formations of rocks. More studies on this topic are needed.

Rock bursts occurred in a tunnel and the mines mentioned in this article have close relation with the characteristic impedance of the rock mass, and the rock bursts happen mostly in the rock masses having high characteristic impedance.

A threshold depth at which the first rock burst occurs exists according to the rock burst data of some mines, and the characteristic impedance at such a depth is defined as critical characteristic impedance.

Laboratory experiments on different rock samples show that seismic velocity increases as applied stress rises, and field monitored results from coal mines indicate that in the areas where rock bursts happened, the seismic velocity was increased markedly before (or during) the bursts.

In rotary drilling, the drillability of rock depends on the characteristic impedance of the rock and the rock with larger impedance has lower drillability or lower penetration rate.

It is possible to evaluate and classify rock mass by characteristic impedance, but this needs validation, especially via field measurements, observations, and other methods.

Declarations

References

Afrouz SG, Westman E, Dehn K, Weston B (2021) Time-dependent monitoring of seismic wave velocity variation associated with three major seismic events at a deep, narrow-vein mine. Min Metall Explor 38:413–426. https://doi.org/10.1007/s42461-020-00327-1

Aladejare AE, Ozoji T, Lawal AI, Zhang ZX (2022) Soft computing-based models for predicting the characteristic impedance of igneous rock from their physico-mechanical properties. Rock Mech Rock Eng. https://doi.org/10.1007/s00603-022-02836-5

Bańka P, Jaworski A (2010) Possibility of more precise analytical prediction of rock mass energy changes with the use of passive seismic tomography readings. Arch Min Sci 55:723–731

Barton N, Lien R, Lunde J (1974) Engineering classification of rock masses for the design of tunnel support. Rock Mech 6(4):189–236. https://doi.org/10.1007/BF01239496

Becquey M, Lavergne M, Willm C (1979) Acoustic impedance logs computed from seismic traces. Geophysics 44(9):1485–1622. https://doi.org/10.1190/1.1441020

Bhandari S (1979) On the role of stress waves and quasi-static gas pressure in rock fragmentation by blasting. Acta Astronaut 6:365–383

Bieniawski ZT (1973) Engineering classification of jointed rock masses. Civil Eng S Afr 15(12). http://worldcat.org/issn/00097845

Bieniawski ZT (1976) Rock mass classification in rock engineering applications. In: Proceedings of the symposium on exploration for rock engineering, vol 12, pp 97–106. https://ci.nii.ac.jp/naid/80014931500/

Bilim N, Karakaya E (2021) Penetration rate prediction models for core drilling. Min Metall Explor 38:359–366

Brauner G (1994) Rockbursts in coal mines and their prevention. AA Balkema, Rotterdam, pp 7–15

Brocher TM (2008) Compressional and shear-wave velocity versus depth relations for common rock types in northern California. Bull Seismol Soc Am 98(2):950–968. https://doi.org/10.1785/0120060403

Brown ET, Hoek E (1978) Trends in relationships between measured in-situ stresses and depth. Int J Rock Mech Min Sci Geomech Abstr 15:211–215

Butel N, Hossack A, Kizil MS (2014) Prediction of in situ rock strength using sonic velocity. In: Proceedings of the coal operators' conference, pp 89–102. https://ro.uow.edu.au/coal/502/

Cai X, Su W, Xu H, He B (2010) Further understanding of the characteristic impedance coupling of explosives to rock. In: Proc.

The 2010 SEG Annual Meeting, Denver. Paper Number: SEG-2010–0137. https://onepetro.org/SEGAM/proceedings-abstract/SEG10/All-SEG10/SEG-2010-0137/96072

Cai W, Dou L, Gong S, Li Z, Yuan S (2015) Quantitative analysis of seismic velocity tomography in rock burst hazard assessment. Nat Hazards 75:2453–2465. https://doi.org/10.1007/s11069-014-1443-6

Cai W, Bai X, Si G, Cao W, Gong S, Dou L (2020) A monitoring investigation into rock burst mechanism based on the coupled theory of static and dynamic stresses. Rock Mech Rock Eng 53:5451–5471. https://doi.org/10.1007/s00603-020-02237-6

Chawre B (2018) Correlations between ultrasonic pulse wave velocities and rock properties of quartz-mica schist. J Rock Mech Geotechn Eng 10(3):594–602

Cook NGW, Hoek E, Pretorius JPG, Ortlepp WD, Salamon MDG (1966) Rock mechanics applied to the study of rockbursts. J S Afr Inst Min Metall 66:435–528

Cooper PW (1996) Explosives engineering. New York: Wiley-Vch

Deere DU (1967) Discussion on rock classification. In: Proceedings of the first congress of the international society for rock mechanics. pp 156–158

Dineva S, Boskovic M (2017) Evolution of seismicity at Kiruna mine. In: Wesseloo J (ed) Proc of eighth international conference on deep and high stress mining, Australian Centre for Geomechanics, Perth, ISBN 978-0-9924810-6-3

Dortman NB (1976). Fiziceskie svoistva gornich porod i polesnich iskopamych. Izdatelstvo Nedra, Moskva

Dou LM, Chen TJ, Gong SY, He H, Zhang SB (2012) Rockburst hazard determination by using computed tomography technology in deep workface. Saf Sci 50(4):736–740

Dou L, Cai W, Gong S, Han R, Liu J (2014) Dynamic risk assessment of rock burst based on the technology of seismic computed tomography detection. J China Coal Soc 39:238–244. https://doi.org/10.13225/j.cnki.jccs.2013.2016(inChinese)

Eaton BA (1969) Fracture gradient prediction and its application in oilfield operations. J Pet Technol 21(10):1353–1360. SPE-2163-PA. https://doi.org/10.2118/2163-PA

Farnfield R, Williams B (2011) Drilling and blasting on the Ty Nant Project. J Explos Eng 28(4):6–17

Feng XT, Liu J, Chen B, Xiao Y, Feng G, Zhang F (2017) Monitoring, warning, and control of rockburst in deep metal mines. Engineering 3:538–545

Gibowicz SJ, Kijko A (1994) An introduction to mining seismology. Academic Press

Gong FQ, Wang YL, Luo S (2020) Rockburst proneness criteria for rock materials: review and new insights. J Cent South Univ 27:2793–2821. https://doi.org/10.1007/s117-y71-020-4511

Goodman RE (1989) Introduction to rock mechanics. Wiley, New York, pp 19–21

Gorbatsevich FF (2014) Density and velocity model of metamorphic rock properties inn the upper and middle crystalline crust in the Kola superdeep borehole (SG-3) section. Acta Geodyn Geomater 11(No.2(174)):165–174

Gorbatsevich FF, Kovalevsky MV, Trishina OM (2011) Characteristics of elastic properties of the crystalline rock samples from the Outokumpu Deep Drill Hole: results of Acoustopolariscopic Laboratory measurements. Geol Surv Finland Spec Pap 51:207–218

He MC, Qian QH (2010) Introduction. In: He MC, Qian QH (eds) The basis of deep rock mechanics. Science Press, Beijing (**in Chinese**)

He J, Dou L, Gong S, Li J, Ma Z (2017) Rock burst assessment and prediction by dynamic and static stress analysis based on microseismic monitoring. Int J Rock Mech Min Sci 93:46–53

He T, Zhao Q, Ha J, Xia K, Grasselli G (2018) Understanding progressive rock failure and associated seismicity using ultrasonic tomography and numerical simulation. Tunn Undergr Space Technol 81:26–34

Hoek E, Kaiser PK, Bawden WF (1995) Support of underground excavations in hard rock. A.A. Balkema, Rotterdam, pp 215

Holma M, Zhang ZX, Kuusiniemi P, Loo K, Enqvist T (2022) Future prospects of muography for geological research and geotechnical and mining engineering. In: Hiroyuki LO, Tanaka KM, Varga D (eds) Muography—exploring earth's subsurface with elementary particles, Wiley

Hosseini N, Oraee K, Shahriar K, Goshtasbi K (2012) Passive seismic velocity tomography on longwall mining panel based on simultaneous iterative reconstructive technique (SIRT). J Cent South Univ 19:2297–2306

Hosseini N, Oraee K, Shahriar K, Goshtasbi K (2013) Studying the stress redistribution around the longwall mining panel using passive seismic velocity tomography and geostatistical estimation. Arab J Geosci 6(5):1407–1416

Howarth DF, Adamson WR, Berndt JR (1986) Correlation of model tunnel boring and drilling machine performances with rock properties. Int J Rock Mech Min Sci Geo Abstr 23(2):171–175

Hudson JA, Harrison JP (1997) Engineering rock mechanics: an introduction to the principles. Pergamon/Elsevier, Oxford

Jaeger JC, Cook NGW, Zimmerman R (2007) Fundamentals of rock mechanics, 4th edn. Wiley-Blackwell, Hoboken

Jia H, Wang E, Song D, Wang X, Ali M (2019) Precursory changes in wave velocity for coal and rock samples under cyclic loading. Res Phys 12:432–434

Jiang L, Kong P, Zhang P, Shu J, Wang Q, Chen L, Wu Q (2020) Dynamic analysis of the rock burst potential of a longwall panel intersecting with a fault. Rock Mech Rock Eng 53:1737–1754. https://doi.org/10.1007/s00603-019-02004-2

Kahraman S, Balcı C, Yazıcı S, Bilgin N (2000) Prediction of the penetration rate of rotary blast hole drills using a new drillability index. Int J Rock Mech Min Sci 37(5):729–743

Kahraman S, Bilgin N, Feridunoglu C (2003) Dominant rock properties affecting the penetration rate of percussive drills. Int J Rock Mech Min Sci 40(5):711–723

Karakus M, Kumral M, Kilic O (2005) Predicting elastic properties of intact rocks from index tests using multiple regression modelling. Int J Rock Mech Min Sci 42(2):323–330. https://doi.org/10.1016/j.ijrmms.2004.08.005

Kerr J (2011) Applications of double-difference tomography for a deep hard rock mine. Dissertation, Virginia Polytechnic Institute, Blacksburg, pp 10–24

Khaksar A, Griffiths CM, McCann C (1999) Compressional- and shear-wave velocities as function of confining stress in dry sandstones. Geophys Prospect 47:487–508

Kolsky H (1963) Stress waves in solids. Dover Publications, New York

Kou S, Rustan A (1993) Computerized design and result prediction of bench blasting. In: Rossmanith H-P (ed) Proc 4th int symp on rock fragmentation by blasting. Balkema, Rotterdam, pp 263–271

Lin W, Wang CW, Geophys JR, astr. SOC (1980) 61, 379–400. P-wave velocities in rocks at high pressure and temperature and the constitution of the central California crust

Lin Y et al (1996) Theory and practice of rock classification. Metallurgical Industry Press, Beijing (**in Chinese**)

Lurka A (2008) Location of high seismic activity zones and seismic hazard assessment in Zabrze Bie-lszowice coal mine using passive tomography. J China Univ Min Technol 18:177–181. https://doi.org/10.1016/S1006-1266(08)60038-3

Ma Y, Liu C, Wu F, Li X (2018) Rockburst characteristics and mechanisms during steeply inclined thin veins mining: a case study in Zhazixi Antimony Mine, China. Shock and Vibration 2018, Article ID 3786047 https://doi.org/10.1155/2018/3786047

Malmgren L, Nordlund E (2006) Behaviour of shotcrete supported rock wedges subjected to blast-induced vibrations. Int J Rock Mech Min Sci 43:593–615

McCulloh TH (1967) Mass properties of sedimentary rocks and gravimetric effects of petroleum and natural gas reservoirs. USGS Professional Paper 528-A, Department of the Interior, United States Geological Survey, Washington, DC. http://pubs.usgs.gov/pp/0528a/report.pdf

Mencacci S, Farnfield R (2003) The measurement and analysis of near-field pressure transients in production blasting. In: Holmberg R (ed) Explosives and blasting technique. Swets & Zeitlinger, Lisse, pp 467–473

Mitri HS, Tang B, Simon R (1999) FE modelling of mining-induced energy release and storage rates. J S Afr Inst Min Metall 2:103–110

Nicholls HR (1962) Coupling explosive energy of rock. Geophysics 27(3):305–316

Nicholls HR, Duvall WI (1963) Effect of characteristic impedance on explosion-generated strain pulses in rock. Rock Mechanics (ed. Fairhurst), Pergamon Press, pp 331

Nordström E, Dineva S, Nordlund E (2017) Source parameters of seismic events potentially associated with damage in block 33/34 of the Kiirunavaara mine (Sweden). Acta Geophys 65:1229–1242. https://doi.org/10.1007/s11600-017-0066-1

Nourani MH, Moghadder MT, Safari M (2017) Classification and assessment of rock mass parameters in Choghart iron mine using P-wave velocity. J Rock Mech Geotech Eng 9(2):318–328

Paithankar AG, Misra GB (1976) A critical appraisal of the Protodyakonov Index. Int J Rock Mech Min Sci Geomech Abstr 13:249–251

Palmström A (1996) Characterizing rock masses by the RMi for use in practical rock engineering: Part 1: the development of the Rock Mass index (RMi). Tunn Undergr Space Technol 11(2):175–188

Rawlings C, Barton N (1995) The relationship between Q and RMR classification in rock engineering. In: Fujill T (ed). In: Proceedings of the 8th international congress on rock mechanics. Minato-Kutokyo Press, Akasaka, pp 29–31

Schön JH (2015) Physical properties of rock, 2nd edn. Elsevier, Oxford

Scott TE, Ma Q, Roegiers JC, Reches Z (1994) Dynamic stress mapping utilizing ultrasonic tomography. Rock Mechanics Models and Measurements Challenges from Industry, Nelson & Laubach, pp 427–434

Simser BP (2019) Rockburst management in Canadian hard rock mines. J Rock Mech Geotechn Eng 11:1036–1043. https://doi.org/10.1016/j.jrmge.2019.07.005

Stålnacke Mats (2022) Private communication on seismic records at the Malmberget mine

Taheri A, Qao Q, Chanda E (2016) Drilling penetration rate estimation using rock drillability characterization index. J Inst Eng India Series D 97(2):159–170

Wang LL (2007) Foundations of stress waves. Elsevier, Oxford

Westman EC (1993) Characterization of structural integrity and stress state via seismic methods: a case study. In: Proceeding of the 12th Conference on Ground Control in Mining, Dep. of Min. Eng., WV Univ., Morgantown, WV, Aug 3–5, 1994, pp 322–329

Whittaker BN, Singh RN, Sun G (1992) Rock fracture mechanics: principles, design and applications. Elsevier, Amsterdam

Williamson ED, Adams LH (1923) Density distribution in the Earth. J Wash Acad Sci 13:413–428. https://www.jstor.org/stable/24532814

Zhang DY (2011) Study on rock burst prediction and control in Jiangbian hydropower station. Master thesis, Shandong University (**in Chinese**)

Zhang ZX (2012) Controlling vibrations caused by underground blasts in LKAB Malmberget mine. Blast Fragm 6(2):63–72

Zhang ZX (2014) Blast-induced dynamic rock fracture in the surfaces of tunnels. Int J Rock Mech Min Sci 71:217–223. https://doi.org/10.1016/j.ijrmms.2014.05.020

Zhang ZX (2016) Rock fracture and blasting: theory and applications. Butterworth-Heinenmann/Elsevier Science, Oxford. https://doi.org/10.1016/C2014-0-01408-6

Zhang ZX, Hou DF (2022) A preliminary investigation of relation between characteristic impedance of rock and penetration rate. In: The 13th International Symposium on Rock Fragmentation by Blasting (FRAGBLAST-13), Hangzhou, China

Zhang ZX, Naarttijärvi T (2005) Reducing ground vibrations caused by underground blasts in LKAB Malmberget mine. Fragblast Int J Blast Fragm 9(2):61–78

Zhang ZX, Hou DF, Aladejare A (2020a) Empirical equations between characteristic impedance and mechanical properties of rocks. J Rock Mech Geotechn Eng 12:975–983. https://doi.org/10.1016/j.jrmge.2020.05.006

Zhang ZX, Enqvist T, Holma M, Kuusiniemi P (2020b) Muography and its potential applications to mining and rock engineering. Rock Mech Rock Eng 53:4893–4907. https://doi.org/10.1007/s00603-020-02199-9

Zhang ZX, Hou DF, Aladejare A, Ozoji T, Qiao Y (2021) World mineral loss and possibility to increase ore recovery ratio in mining production. Int J Min Reklam Env 35(9):670–691. https://doi.org/10.1080/17480930.2021.1949878

Zhao MJ, Wu DL (2000) Ultrasonic classification and strength prediction of engineering rock mass. Chin J Rock Mech Eng 19(1):89–92 http://www.rockmech.org/CN/Y2000/V19/I01/89 (**in Chinese**)

Zhou J, Li X, Mitri HS (2018) Evaluation method of rockburst: state-of-the-art literature review. Tunn Undergr Space Technol 81:632–659

Zou D (2017) Theory and technology of rock excavation for civil engineering. Springer jointly published with Metallurgical Industry Press, Singapore. https://doi.org/10.1007/978-981-10-1989-0